BILINGUAL PUBLISHING GROUP

Journal of Environmental & Earth Sciences

https://journals.bilpubgroup.com/index.php/jees

SHORT COMMUNICATION

CH_4 Decomposition to Green H_2 over PM(1wt%)-Ni(20wt%)/MCM-41 (PM = Pd, Pt, and Rh) Catalysts

Ho Joon Seo

Department of Chemical and Biomolecular Engineering, Chonnam National University, Yeosu 59626, Republic of Korea

ABSTRACT

The CH_4 is a greenhouse gas with a global warming potential(GWP) 21 times greater than CO_2. The catalytic decomposition of CH_4 (CDM) is a climate-friendly, CO_2-free process that produces only green H_2 and carbon nanomaterials such as carbon nanotubes. The CDM to green H_2 over PM(1wt%)-Ni(20wt%)/MCM-41 (PM = Pd, Pt, and Rh) catalysts was investigated using a packed-bed flow reactor(PBFR) under atmospheric pressure. The catalysts were characterized through XPS and XRD. XRD analysis revealed that NiPd crystallites were formed owing to appropriate interactions between Ni^{2+} and Pd^{2+}. XPS analysis revealed that adding of 1 wt% of Pd to Ni(20wt%)/MCM-41 increased the Ni2p atomic percentage of Pd(1wt%)-Ni(20wt%)/MCM-41 from 2.77% to 4.27%, and decreased that of O1s the from 68.59% to 66.92%. The core electron levels, such as Ni2p, O1s, and Si2p in fresh Pd(1)-Ni(20)/MCM had a slight chemical shift toward lower energy compared to those of Ni(20wt%)/MCM-41. The H_2 yield on the Pd(1 wt%)-Ni(20wt%)/MCM-41 is much higher than that of PM(1wt%)-Ni(20wt%)/MCM-41 (PM = Pt, Rh) and Ni(20wt%)/MCM-41 even after 1.2×10^4 s of CDM, while that of Ni(20wt%)/MCM-41 decreased rapidly. The H_2 yield of Pd(1wt%)-Ni(20wt%)/MCM-41 in CDM was enhanced owing to the increased Ni2p distribution and the enhanced reduction degree caused by H_2 spillover via appropriate metal-carrier interaction (AMCI) between Pd, Ni, and MCM-41. The CDM is an environmentally friendly process that produces COx-free and economical green H_2 by using a catalyst of 1 wt% Pd onto Ni(20wt%)/MCM-41.

Keywords: Green H_2; Global Warming Mitigation; Climate Change; Clean Energy; CH_4 Decomposition

*CORRESPONDING AUTHOR:

Ho Joon Seo, Department of Chemical and Biomolecular Engineering, Chonnam National University, Yeosu 59626, Republic of Korea; Email: hjseo@jnu.ac.kr

ARTICLE INFO

Received: 31 May 2025 | Revised: 23 June 2025 | Accepted: 28 June 2025 | Published Online: 24 July 2025
DOI: https://doi.org/10.30564/jees.v7i7.10292

CITATION

Seo, H.J., 2025. CH_4 Decomposition to Green H_2 over PM(1wt%)-Ni(20wt%)/MCM-41 (PM = Pd, Pt, and Rh) Catalysts. Journal of Environmental & Earth Sciences. 7(7): 334–340. DOI: https://doi.org/10.30564/jees.v7i7.10292

1. Introduction

As the concentration of CH_4 in the atmosphere increases owing to human activities such as the use of fossil fuels, agriculture, and landfills, climate change is changing, seriously affecting the global environment such as weather phenomena, rising sea levels, and changes in marine ecosystems. The IPCC report[1] emphasizes that carbon neutrality requires a strong reduction in not only carbon dioxide but also other greenhouse gas emissions such as CH_4. The CDM has attracted significant attention as a promising alternative for climate-friendly green H_2 without greenhouse gas emissions, such as CO_x and NO_x[2]. On the other hand, the steam reforming (SMR) and partial oxidation of CH_4(POM) to grey H_2 emit a lot of greenhouse gases, namely CO_x, CO and CO_2, which have a serious greenhouse effect on the Earth. The CH_4 is a greenhouse gas with a GWP[3] 21 times greater than CO_2. Also, the CH_4 is the main component of natural gas and is endothermic, as shown in equation (1). It only produces green H_2 and nanocarbon materials without emitting CO_x. However, the implementation of CDM is challenging owing to its energy-intensity and thermodynamic tendency toward carbon deposition, which causes catalyst deactivation.

$$CH_4 \rightarrow C + 2H_2, \quad \widehat{\Delta H}_r^0 = 75.6 \text{ kJ/mol} \qquad (1)$$

The precious metals, such as palladium, platinum, and rhodium are effective in maintaining high activity and stability in CDM, but they are unsuitable owing to high cost and scarcity in terms of industry. Using group VIII 3d transition metal, nickel(Ni) offers an industrially viable alternative, providing both low cost and high availability[4, 5]. It exhibits excellent initial catalytic activity but is prone to rapid carbon deposition on the catalyst surface, leading to catalyst deactivation. Various strategies have been explored to extend the lifespan of Ni catalysts and mitigate carbon deposition on the catalyst surface[6]. Takriff et al.[7] report that adding Pt to Ni/CeO_2 enhances the activity and stability in CDM reaction by lowering the NiO reduction temperature through H_2 spillover while improving the uniform distribution of fine particles on the catalyst through moderate metal-carrier interaction. Dai et al.[8] report that the appropriate addition of precious metal promoters such as Pd, Pt, and La to a Ni-based catalyst in CDM for H_2 increases catalyst activity and prevents carbon deposition on the catalyst. Millar et al.[9] report that MCM-41, with pore sizes ranging from 2 nm to 50 nm in a uniform hexagonal structure, is widely used as a catalyst carrier and adsorbent because of its physical properties, including thick walls and high thermal stability.

This study aims to investigate the effect of platinum-group metals(PM)(Pd, Pt, and Rh) as promoters to develop a catalyst with sustained high activity and long-term stability. In terms of economic feasibility and efficiency for producing green H_2 under CDM. The catalysts used were characterized by X-ray Photoelectron Spectroscopy (XPS) and X-ray Diffraction(XRD). They evaluated through catalyst performance tests in CDM using a PBFR under atmospheric pressure for green H_2.

2. Materials and Methods

2.1. Catalyst Preparation

PM(1wt%)-Ni(20wt%)/MCM-41 (PM = Pd, Pt, and Rh) catalysts were prepared using a standard support method. Ethanol(99.9%, Daejung, South Korea) was added to the reactor, followed by dissolving 2.0×10^{-6} kg each of $Pd(NO_3)_2 \cdot xH_2O$(Aldrich), $Pt(NO_3)_2 \cdot xH_2O$(Aldrich), $Rh(NO_3)_2 \cdot xH_2O$(Aldrich), alongside 3.0×10^{-4} kg of $Ni(NO_3)_2 \cdot 6H_2O$(Aldrich) in ethanol. Subsequently, 1.0×10^{-4} kg of MCM-41 (Aldrich) was added, and the mixture was stirred uniformly for 1.8×10^4 s. The resulting precipitate was filtered and dried in a dryer at 373K for 8.6×10^4 s. The dried sample was calcined at 773 K for 1.8×10^4 s in an electric furnace (Eyela, TMF-1000) to create PM(1wt%)-Ni(20wt%)/MCM-41 (PM = Pd, Pt, and Rh), Ni(20wt%)/MCM-41, and Pt(1 wt%)/MCM-41 catalyst. The calcined sample was then ground to 150–200 mesh for use.

2.2. Catalyst Characterization

XRD pattern was obtained using a Panalytical Empyrean 3D high-resolution X-ray diffractometer with Cu Kα radiation(λ = 1.5419 Å; 40 kV, 30 mA). XPS Spectra were acquired using Alkα X-rays under operating conditions of 1×10^{-9} mbar and 1.75 keV with an HP-X-ray photoelectron spectrometer (Thermo Scientific K-Alpha+).

2.3. Catalyst Performance

The CDM to H_2 was performed using a PBFR under atmospheric pressure with process stability and energy reduction effects. A 5.0×10^{-5} kg of powdered catalyst was placed on quartz cotton within a quartz reactor with a 1.0×10^{-2} m internal diameter and 0.3 m length. Subsequently, pure CH_4(99.999%, Samjung Co., South Korea) was supplied to the reactor at a gas hourly space velocity(GHSV) of 1.2×10^{-2} CH_4 mL/$kg_{cat.}$·s under reaction conditions of 973K and 101.3 kPa. The reactor temperature was controlled within ±1K using a PID controller with a K-type thermocouple placed on the catalyst in the reactor. After purging the reactant through a pressure gauge attached to each cylinder, the reactant composition was regulated with a mass flow controller(Aalborg, USA). The product was analyzed using a thermal conductivity detector with a Molecular sieve 5 A column connected to a Gas chromatograph (Shimadzu Co., Model 14B, Japan). Before the reaction, the catalyst was employed by reducing the H_2 temperature to 773 K for 1.8×10^4 s at 3.3×10^{-1} ml/s flow rate, then increasing the reaction temperature at a rate of 4.7 K/s. The data were used as an average value obtained by performing three to five experiments. The H_2 yield for each catalyst was calculated using the following equation:

$$H_2 \text{ yield } (\%) = \frac{\text{moles of } H_2 \text{ produced}}{2 \times \text{moles of } CH_4 \text{ in the feed}} \times 100 \quad (2)$$

3. Results and Discussion

3.1. Catalyst Activity

Figure 1 illustrates the H_2 yield vs. reaction time for CDM over the PM(1wt%)-Ni(20wt%)/MCM-41 (PM = Pd, Pt, and Rh), Ni(20wt%)/MCM-41, and Pt(1)/MCM-41 catalysts. The H_2 yield for the Pd(1wt%)-Ni(20wt%)/MCM-41 catalyst remained relatively constant, averaging approximately 62.1%. However, the H_2 yield for the Rh(1 wt%)-Ni(20wt%)/MCM-41 catalyst initially stabilized, reaching about averagely at approximately 60.8% but declined rapidly, reaching 23.6% at 1.6×10^4 s. The H_2 yield for the Pt(1wt%)-Ni(20wt%)/MCM-41 catalyst was initially lower than that of the Ni(20wt%)/MCM-41 catalyst until 8.3×10^3 s; however, after that, the Pt(1wt%)-Ni(20wt%)/MCM-41 catalyst showed a significantly higher H_2 yield than that of the Ni(20wt%)/MCM-41 catalyst. Moreover, the H_2 yield for the Ni(20wt%)/MCM-41 catalyst decreased continuously, reaching 29.1% at 1.2×10^4 s. Additionally, the H_2 yield for Pt(1wt%)/MCM-41 catalyst continued to increase until 2.7×10^3 s, reaching 55.2%, but decreased rapidly after that, dropping to 22.3% at 1.7×10^4 s.

This phenomenon is owing to a lot of carbon deposition[10] on the Ni(20wt%)/MCM-41 catalyst surface and sintering of Ni particles caused by the low Tammann temperature. The addition of 1 wt% PM (Pd, Pt, and Rh) as a promoter to Ni(20wt%)/MCM significantly affected the H_2 yield of CDM. The H_2 yield of Pd(1wt%)-Ni(20wt%)/MCM-41 was approximately 1.5 times higher than that of Ni(20wt%)/MCM-41. The H_2 yield of the catalysts used in CDM at 1.2×10^4 s followed the order — Pd(1wt%)-Ni(20wt%)/MCM-41 ≫ Pt(1wt%)-Ni(20wt%)/MCM-41 > Rh(1wt%)-Ni(20wt%)/MCM-41 > Ni(20wt%)/MCM-41 ≫ Pt(1 wt%)/MCM-41. The H_2 yield is assumed to be improved by Ni2p distribution[7] owing to appropriate metal-carrier interactions among the PM (Pd, Pt, and Rh), Ni, and MCM-41 alongside increased reduction degree, which causes H_2 spillover[11]. Otsuka et al.[12] reported that CDM was performed on an M-Ni (5 wt%) (M = Pd, Pt, Rh) catalyst at a reaction temperature of 823 K and an M/Ni molar ratio of 0.1, and that adding Rh and Pt to Ni (5 wt%)/SiO_2 shortened the catalyst life, but adding Pd improved it. Economical green H_2 can be produced by using catalyst of 1 wt% Pd onto Ni(20wt%)/MCM-41 in the CDM process.

3.2. Characterization of Fresh Pd(1wt%)-Ni(20wt%)/MCM-41 Catalyst

Figure 2 displays the XRD patterns of fresh Pd(1wt%)-Ni(20wt%)/MCM-41 catalyst reduced before reaction. Characteristic peaks of NiO at 2θ = 44.53° and them of cubic Ni were observed at 2θ = 51.89° and 76.38°, showed the presence of NiO(2 0 0)[6], Ni(2 0 0), Ni(2 2 0) planes (JCPDS: 03-1051), respectively, alongside those of cubic NiPd at 2θ = 41.69°, 45.18° ,showed the presence of NiPd(1 1 1), NiPd(2 2 0) planes[13], respectively. However, no characteristic peaks for Pd were detected. These results suggest the NiPd crystallites formation, indicating an appropriate interaction between Ni^{2+} and Pd^{2+}.

It is believed that the NiPd crystalline phase will affect high H_2 yield and catalyst stability[13].

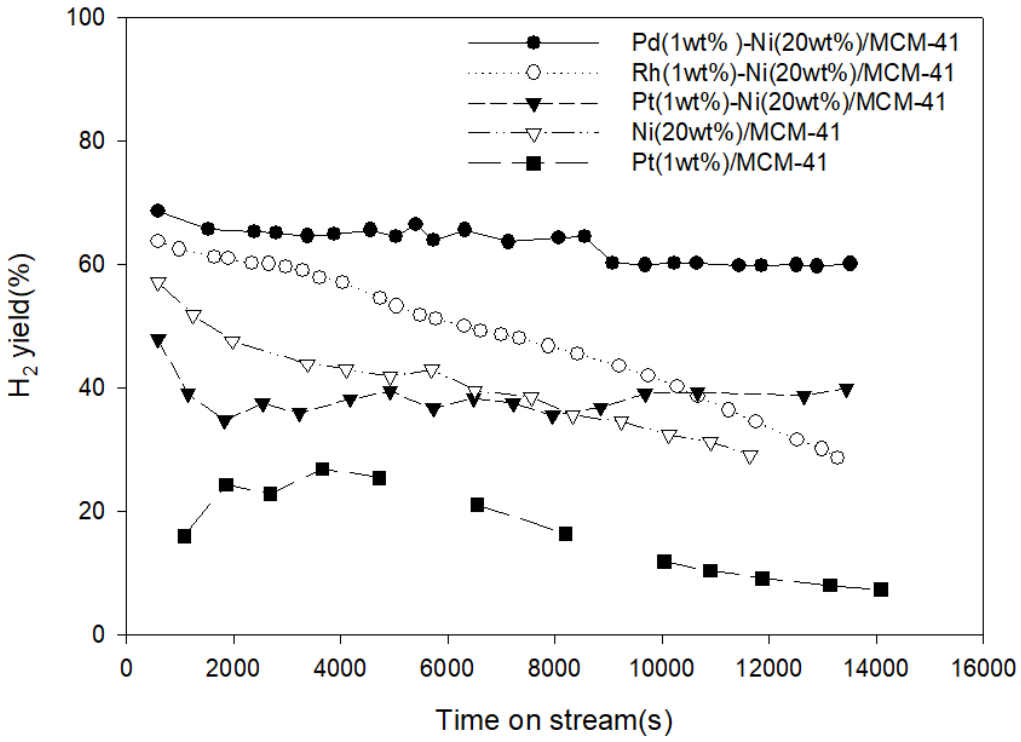

Figure 1. H_2 yield from CH_4 decomposition over PM(1wt%)-Ni(20wt%)/MCM-41 (PM = Pd, Pt, and Rh), Ni(20wt%)/MCM-41, and Pt(1wt%)/MCM-41 in a PBFR under the following conditions: P = 101.3 kPa, T = 973K, and GHSV = 1.2×10^{-2} CH_4 mL $kg_{cat.}^{-1}$ s^{-1}.

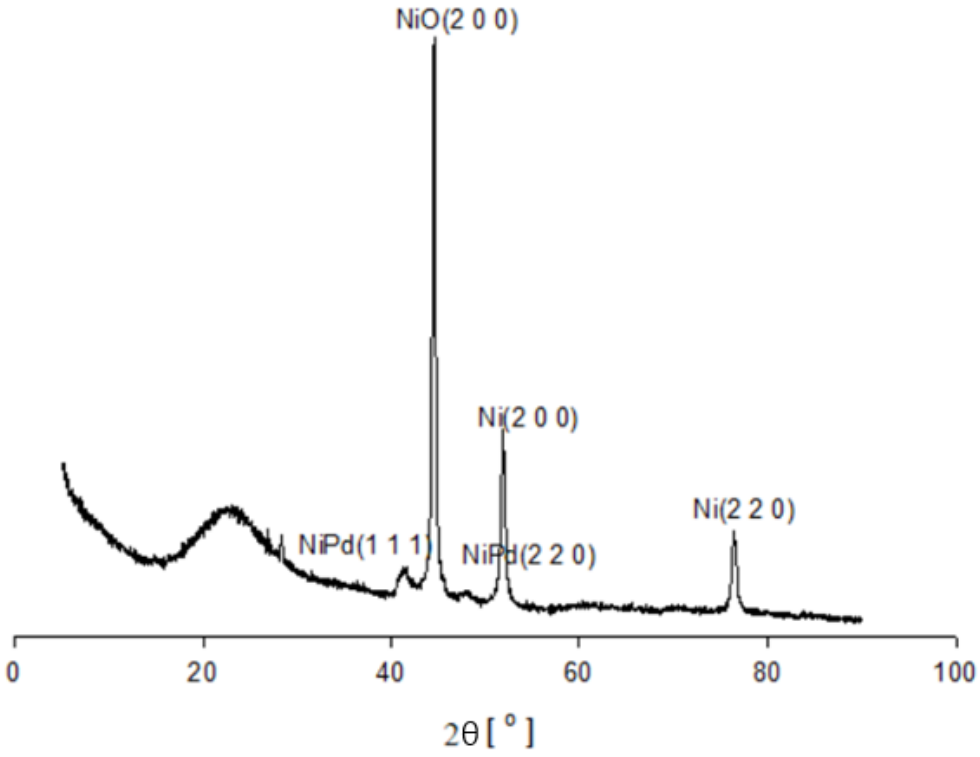

Figure 2. Standard XRD patterns of fresh Pd(1wt%)-Ni(20wt%)/MCM-41.

Table 1 presents the atomic percentage of core electron levels for fresh Pd(1wt%)-Ni(20wt%)/MCM-41 and Ni(20wt%)/MCM-41 catalyst reduced before reaction, as determined via XPS. The addition of 1 wt% of Pd to the Ni(20wt%)/MCM-41 catalyst increases the atomic percentage of Ni2p from 2.77% to 4.27%, while that of O1s decreases from 68.59% to 66.92%. The 1.50% increase in Ni2p atomicity on Pd(1wt%)-Ni(20wt%)/MCM-41 surface is attributed to the appropriate metal-support interaction among Ni, Pd, and MCM-41, indicating high dispersion of Ni particles. The atomic percentage of O1s core electron levels, including lattice oxygen and oxygen vacancies of the Pd(1wt%)-Ni(20wt%)/MCM-41 was 1.02 times lower than that of the Ni(20wt%)/MCM-41. This indicates that some of the lattice oxygens(O^{2-}) in MCM-41 were replaced by oxygen vacancy(O^{-}) through mutual substitution of Pd^{2+} (86 pm), Ni^{2+} (135 pm), and Si^{4+} (110 pm) with different ionic radii. In addition, it has been suggested that the formation of Pd-s-Si^{3+} may be found on the catalytic surface by electron transfer from Si to Pd due to electronegativity, where denotes an oxygen defect vacancy. The atomic percentage of Pd3d is 0.04.

Table 1. Atomic percentage of core electron levels in fresh Pd(1wt%)-Ni(20wt%)/MCM-41 and Ni(20wt%)/MCM-41 based on XPS data.

Fresh Catalyst	Core Electron Levels	Atomic%
Pd(1wt%)-Ni(20wt%)/MCM-41	O1s	66.92
	Si2p	28.76
	Ni2p	4.27
	Pd3d	0.04
Ni(20wt%)/MCM-41	O1s	68.59
	Si2p	28.64
	Ni2p	2.77

This phenomenon is believed to enhance Ni2p dispersion owing to the appropriate metal-support interaction [8] by substituting some of Si^{4+} in SiO_2 with Ni^{2+} or Pd^{2+} ions and oxygen vacancy formation — thereby maintaining the activity and stability and of Pd(1wt%)-Ni(20wt%)/MCM-41.

Figure 3 shows the XPS spectra of (a) Ni2p, (b) O1s, (c) Pd3d, and (d) Si2p core electron levels for fresh Ni(20wt%)/MCM-41 and Pd(1wt%)-Ni(20wt%)/MCM-41 catalysts reduced before the reaction. The characteristic $Ni2p_{3/2}$ peaks for fresh Pd(1wt%)-Ni(20wt%)/MCM-41, namely Ni^{0}, Ni^{2+}, and satellite, appeared at 850.28, 855.18, and 860.58 eV, respectively. $Ni2p_{1/2}$ peak, namely Ni^{2+} and satellite, appeared at 872.58 and 879.08 eV, respectively. For fresh Ni(20wt%)/MCM-41, the $Ni2p_{3/2}$ peaks, namely Ni^{o}, Ni^{2+}, and satellite, appeared at 852.1, 855.31, and 860.88 eV, while the $Ni2p_{1/2}$ peaks, namely Ni^{2+} and satellite, appeared at 873.08 eV and 880.08 eV, respectively. The characteristic O1s peak for fresh Ni(20wt%)/MCM-41 appeared at 531.28 eV, while that for fresh Pd(1wt%)-Ni(20wt%)/MCM-41, corresponding to Si–O-Si binding energy exhibited a slight chemical shift toward lower energy than Ni(20wt%)/MCM-41. The O^{2-} and O^{-} peaks of fresh Ni(20wt%)/MCM-41 appeared at 532.58 and 532.86 eV, respectively. While those of fresh Pd(1wt%)-Ni(20wt%)/MCM-41 appeared at 532.11 and 532.68 eV, respectively, showing a slight chemical shift toward lower energy than Ni(20wt%)/MCM-41. Characteristic $Pd3d_{5/2}$ peak for fresh Pd(1 wt%)-Ni(20wt%)/MCM-41, namely Pd^{0}, appeared at 334.58 eV, while $Pd3d_{3/2}$ peak, namely Pd^{0}, appeared at 339.58 eV. Characteristic Si2p peak for fresh Pd(1wt%)-Ni(20wt%)/MCM-41, namely Si^{+4}, appeared at 103.21 eV, while fresh Ni(20wt%)/MCM-41 peak appeared at 103.72 eV. Compared to fresh Ni(20wt%)/MCM-41, the core electron levels such as Ni2p, O1s, and Si2p of fresh Pd(1wt%)-Ni(20wt%)/MCM-41 exhibited a slight chemical shift toward lower energy. Addition 1 wt% of Pd to the Ni(20wt%)/MCM-41 shifts binding energy of the core electrons level toward lower energy than Ni(20wt%)/MCM-41, probably owing to the charge transfer from Si to Pd and the change in the SiO_2 lattice by NiPd alloy formation. In addition, the Pd^{0} is able to activate from CH_4 to H_2, then decrease the binding energy by favouring the reduction of Ni ions by H_2 spillover. Dogu et al. [6] reported that the addition of 0.5 wt% of Pd to Ni/MCM-41 improves the dispersion of Ni particles on the catalyst surface, and creates small nano-sized Ni particles, which easily reduce NiO particles.

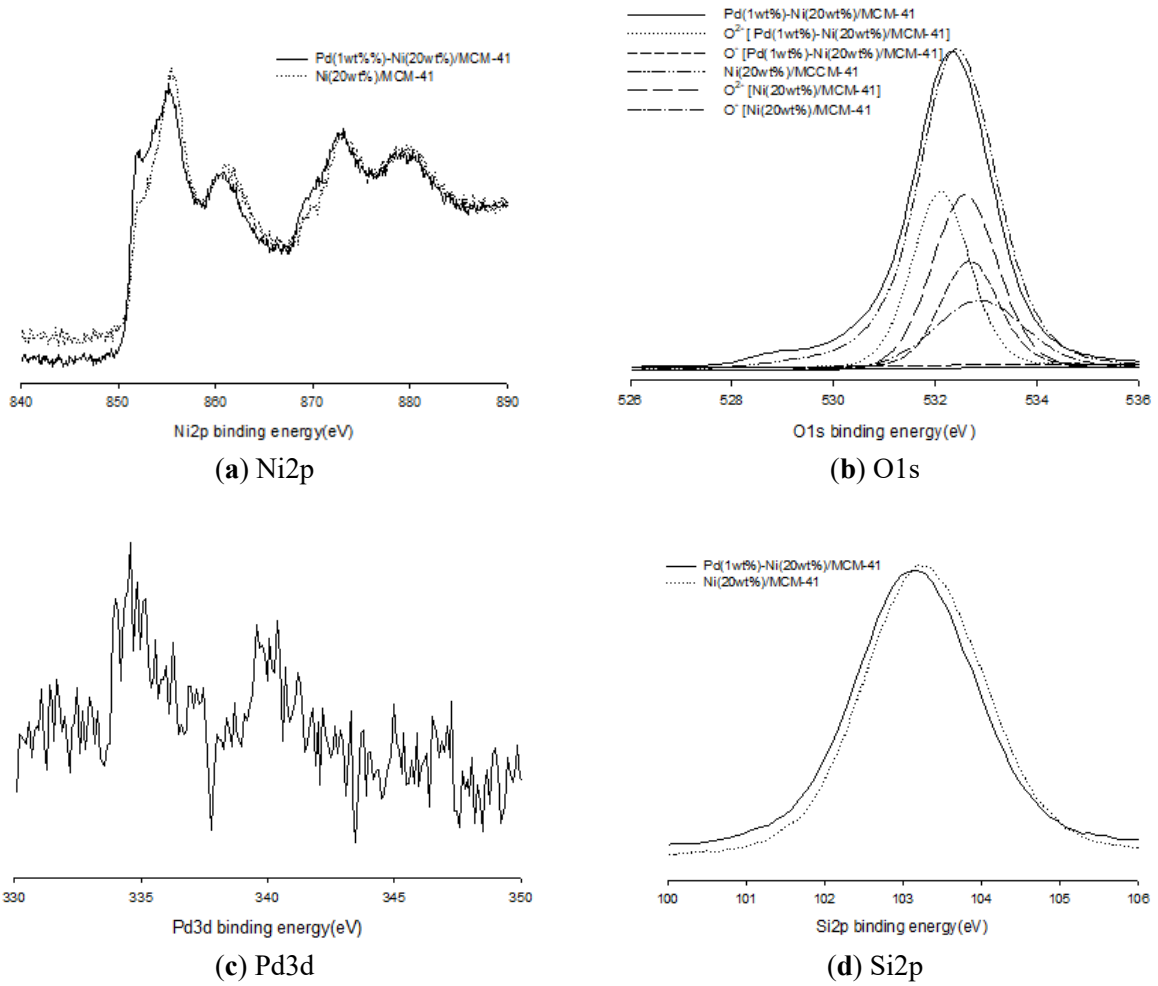

Figure 3. XPS spectra showing (**a**) Ni2p, (**b**) O1s, (**c**) Pd3d, (**d**) Si2p core electron levels for fresh Pd (1wt%)-Ni (20wt%)/MCM-41 and fresh Ni (20wt%)/MCM-41.

These findings suggest that Ni ions in Pd(1wt%)-Ni(20wt%)/MCM-41 were more readily reduced owing to H_2 spillover compared to those in Ni(20wt%)/MCM-41, and the dispersion is enhanced on the catalyst surface owing to the appropriate metal-support interaction, where some Si^{4+} in SiO_2 is substituted with Ni^{2+} or Pd^{2+} ions.

4. Conclusions

The H_2 production was achieved by performing CDM over PM(1wt%)-Ni(20wt%)/MCM-41 (PM = Pd, Pt, and Rh), Ni(20wt%)/MCM-41, and Pt(1wt%)/MCM-41 using a PBFR under atmospheric conditions. The addition of 1 wt% PM (Pd, Pt, and Rh) as a promoter to Ni(20wt%)/MCM significantly affected of CDM to H_2 yield. Pd(1wt%)-Ni(20wt%)/MCM-41 achieved approximately 1.5 times higher H_2 yield than that of Ni(20wt%)/MCM-41. At 1.2×10^4 s, the H_2 yield of catalysts in CDM followed the order of Pd(wt%1)-Ni(20wt%)/MCM-41 $\gg$ Pt(1wt%)-Ni(20wt%)/MCM-41 $>$ Rh(1wt%)-Ni(20wt%)/MCM-41 $>$ Ni(20wt%)/MCM-41 $\gg$ Pt(1wt%)/MCM-41. The NiPd crystallites formed through appropriate interaction between Ni^{2+} and Pd^{2+} ions promoted Ni2p enrichment on the MCM-41 surface, supporting the H_2 yield and stability of Pd(1wt%)-Ni(20wt%)/MCM-41. The Ni2p atomic percentage in Pd(1wt%)- Ni(20wt%)/MCM-41 also increased from 2.77% to 4.27% compared to that in Ni(20wt%)/MCM-41, while that of O1s decreased from 68.59% to 66.92%. The Ni2p, O1s, and Si2p core electron levels in fresh Pd(1wt%)-Ni(20wt%)/MCM-41 exhibited a slight chemical shift toward lower energy compared to those of Ni(20wt%)/MCM-41. Compared to Ni(20wt%)/MCM-41, the Pd(1wt%)-

Ni(20wt%)/MCM-41 is believed to increase Ni2p distribution owing to the appropriate metal-support interaction and earlier reduction from H_2 spillover, thereby maintaining the H_2 yield and the catalyst stability. The CDM is an environmentally friendly process that produces CO_x-free H_2 rather than the POM and the SMR. In addition, economical green H_2 can be produced by using a catalyst of 1 wt% Pd onto Ni(20wt%)/MCM-41 in the CDM process.

Funding

This research received no external funding.

Institutional Review Board Statement

Not applicable.

Informed Consent Statement

Not applicable.

Data Availability Statement

Data are contained within the article.

Conflicts of Interest

The authors declare no confict of interest, financial or otherwise.

References

[1] IPCC, 2022. The evidence is clear: the time for action is now. We can halve emissions by 2030. 6th April 4, 2022.

[2] Abbas, H.F., Daud, W.M.A., 2010. Hydrogen production by methane decomposition: A review. International Journal of Hydrogen Energy. 35(3), 1160–1190. DOI: https://doi.org/10.1016/j.ijhydene.2009.11.036

[3] Yusuf, R.O., Noor, Z.Z., Abba, A.H., Hassan, M.A.A., Din, M.F.M., 2012. Methane emission by sectors: A comprehensive review of emission sources and mitigation methods. Renewable and Sustainable Energy Reviews. 16(7), 5059–5057. DOI: https://doi.org/10.1016/j.rser.2012.04.008

[4] Yao, Y., Liu, X., Hildebrandt, D., and Glasser, D., 2011. Fisher-Tropsch synthesis using $H_2/CO/CO_2$ syngas mixtures over an iron catalyst. Industrial & Engineering Chemistry Research. 50(19), 11002–11012. DOI: https://doi.org/10.1021/ie200690y

[5] Awadallah, A.E., Aboul-Enein, A.A., El-Desouki, D.S., et al., 2014. Catalytic thermal decomposition of methane to COx-free hydrogen and carbon nanotubes over MgO supported bimetallic group VIII catalysts. Applied Surface Science. 96, 100–107. DOI: https://doi.org/10.1016/j.apsusc.2014.01.055

[6] Damyanova, S., Pawelec, B., Arishtirova, K., et al., 2009. MCM-41 supported PdNi catalysts for dry reforming of methane. Applied Catalysis B: Environmental. 92, 250–261. DOI: https://doi.org/10.1016/j.apcatb.2009.07.032

[7] Pudukudy, M., Yaakob, Z., Jia, Q., et al., 2018. Catalytic decomposition of undiluted methane into hydrogen and carbon nanotubes over Pt promoted Ni/CeO2 catalysts. New Journal of Chemistry. 42, 14843–14856. DOI: https://doi.org/10.1039/C8NJ02842G

[8] Karimi, S., Fatemeh, B., Meshkani, F., et al., 2021. Promotional roles of second metals in catalyzing methane decomposition over the Ni-based catalysts for hydrogen production: A critical review. International Journal of Hydrogen Energy. 46, 20435–20480. DOI: https://doi.org/10.1016/j.ijhydene.2021.03.160

[9] Zhao, X.S., Lu, G.Q., Millar, G.J., 1996. Advances in mesoporous molecular sieve MCM-41. Industrial & Engineering Chemistry Research. 35(7), 2075–2090. DOI: https://doi.org/10.1021/ie950702a

[10] Seo, H.J., 2024. Catalytic decomposition of CH4 to hydrogen and carbon nanotubes using the Pt(1)-Fe(30)/MCM-41 catalyst. Catalysts. 14(4), 282–301. DOI: https://doi.org/10.3390/catal14040282

[11] Guo, J.-H., Li, X.-D., Cheng, X.-L., Liu, H.-Y., Li, S.-J., Chen, G., 2018. The theoretical study of the bimetallic Ni/Pd, Ni/Pt and Pt/Pd catalysts for hydrogen spillover on penta-graphene. International Journal of Hydrogen Energy. 43, 19121–19129. DOI: https://doi.org/10.1016/j.ijhydene.2018.08.143

[12] Takenaka, S., Shigeta, Y., Tanabe, E., Otsuka, K., 2003. Methane decomposition into hydrogen and carbon nanofibers over supported Pd-Ni catalysts. Journal of Catalysis. 220, 468–477. DOI: https://doi.org/10.1016/S0021-9517(03)00244-6

[13] Li, P., Li, F., Deng, G., Guo, X., Liu, H., Jiang, W., Wang, T., 2016. Polymerized-complex method for preparation of supported bimetallic alloy and monometallic nanoparticles. Chemical Communications. 52, 2996–2999. DOI: https://doi.org/10.1039/C5CC08848H